Two-dimensional intrinsic and extrinsic ferromagnetic behavior of layered $La_{1.2}Sr_{1.8}Mn_2O_7$ single crystals

C. D. Potter,* Maribeth Swiatek,† and S. D. Bader
Materials Science Division, Argonne National Laboratory, Argonne, Illinois 60439

D. N. Argyriou‡
Science and Technology Center for Superconductivity, Argonne National Laboratory, Argonne, Illinois 60439

J. F. Mitchell, D. J. Miller, D. G. Hinks, and J. D. Jorgensen
Materials Science Division and Science and Technology Center for Superconductivity, Argonne National Laboratory, Argonne, Illinois 60439

(Received 16 June 1997)

The low-field magnetization M and susceptibility χ are reported for the two-layered Ruddleson-Popper phase $SrO(La_{1-x}Sr_xMnO_3)_2$ for $x=0.4$ (denoted $La_{1.2}Sr_{1.8}Mn_2O_7$) with an in-plane magnetic easy axis. As T approaches the Curie temperature ($T_C=116$ K) on cooling, where the metal-insulator transition occurs in zero field, χ diverges as $H^{-1/\delta'}$, with $\delta=21\pm5$. Also, near an extrinsic Curie transition attributed to ~0.1% volume fraction of intergrowths at $T^*=2.47\ T_C$, M scales as $(1-T/T)^{\beta}$, with $\beta=0.25\pm0.02$. These results can be understood within the context of two-dimensional XY models, and provide some perspective of the layered manganites. [S0163-1829(98)02102-X]

The revival of interest in manganite perovskites is driven by the observation of colossal magnetoresistance (CMR) effects.[1–4] The CMR can be understood at an elementary level within the context of double-exchange theory[5] as a field-enhanced metal-insulator (MI) transition at the Curie temperature T_C. Within this framework the singly occupied e_g level of the high-spin Mn^{+3} state lies above the triply occupied t_{2g} level and can be Jahn-Teller split due to the lowering of the octahedral symmetry of the oxygen ligands. The e_g electron can hop across an oxygen site in a spin-conserving manner (double-exchange process) to the corresponding unoccupied e_g level of a neighboring Mn^{+4} site *if the two sites are spin aligned.* Hence, the e_g electron can delocalize at T_C, which is where all the Mn sites spin align. This is, however, an oversimplification and much of the physics of the CMR materials still needs to be elucidated, including the role of polaronic conduction, and the micromagnetic understanding of the lack of significant remanence reported for these materials.[3,6]

Recently, layered variants of the perovskite structure, analogous to the layered cuprates, have been explored with the expectation that they will provide new insights and interesting physics in their own right due to unique anisotropies and dimensionality effects.[7–10] For example, $La_{1.2}Sr_{1.8}Mn_2O_7$ was introduced by Moritomo *et al.*[7] who identified its concomitant Curie and MI transitions and CMR at T_C~120 K, and short-range order (SRO) above T_C. The structure remains tetragonal ($I4/mmm$) throughout the transitions and consists of an insulating blocking layer separating two conducting manganese-oxide layers, as represented by the formula $SrO(La_{1-x}Sr_xMnO_3)_n$ with $x=0.4$ and $n=2$. [The structure evolves into that of the three-dimensional (3D) perovskites as n increases to infinity.] For $x=0.4$, the resistivity vs temperature at the MI transition reverses slope and drops on cooling by two orders of magnitude for both the current in the ab plane ρ_{ab}, and the current perpendicular to the plane, ρ_c.[8] Subsequently, Kimura *et al.*[10] studied the $x=0.3$ member of this series and reported that the c axis is the easy axis, and that the resistivity behavior is different than for the $x=0.4$ material: ρ_{ab} underwent its slope reversal at an elevated temperature that we will denote T^*, while ρ_c plummeted at T_C (~90 K). From the observations in Ref. 10 a picture emerged that incorporates the following elements: (i) there are two transitions, (ii) they are both intrinsic, (iii) the upper transition is due to double-exchange coupling within the layers, and (iv) the lower transition is due to interplanar tunneling. In the present work we examine the $x=0.4$ material and also find two transitions, as for the $x=0.3$ material, but we differ with Ref. 10 concerning points (ii)–(iv) above. We find that the a axis is the easy axis in our material, and that although there are two transitions, the upper transition at T^* is extrinsic and attributed to trace amounts of intergrowths, identified via transmission electron microscopy (TEM), and as are also known to occur in the layered cuprates. Thus, we conclude that it is the Curie transition at T_C that is dominated by double-exchange considerations. Quantitatively, we also find unusual scaling of both the low-field susceptibility near the intrinsic transition at T_C, *and* of the magnetization with temperature below the extrinsic transition at $T^*=2.47\ T_C$ for the impurities (intergrowths) that represent only ~0.1% volume fraction of the sample.

The synthesis and neutron-scattering structural determinations of our samples have been described previously.[8,9] Single crystals of $La_{1.2}Sr_{1.8}Mn_2O_7$ were prepared from powders of the oxides and grown in a floating-zone image furnace in flowing oxygen.[8] This yielded a boule about 1 cm in diameter and 8 cm in length that contained many single crys-

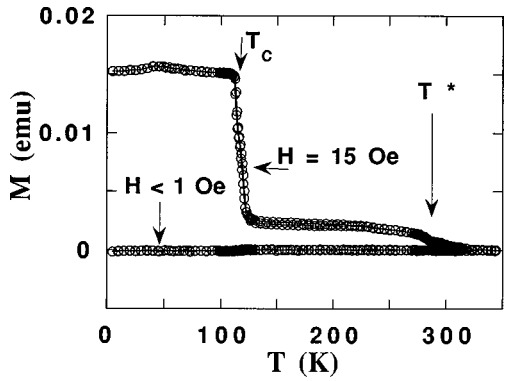

FIG. 1. M vs T for $La_{1.2}Sr_{1.8}Mn_2O_7$ measured with H parallel to the a axis. T_C and T^* identify intrinsic and extrinsic Curie transitions, respectively.

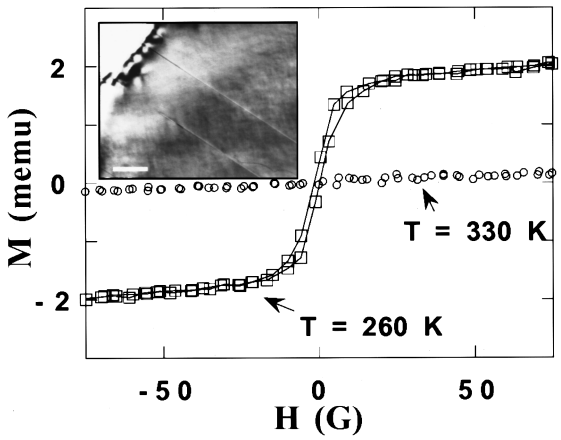

FIG. 2. M vs H for $La_{1.2}Sr_{1.8}Mn_2O_7$ below (260 K) and above (330 K) T^*. The inset shows a TEM micrograph with a 50-nm scale marker. This image thus contains about one intergrowth for every 2000 Å.

tals. Crystals from parts of the boule were crushed into a powder for neutron-diffraction measurements,[9] while the remaining single crystals were used for magnetometry and magnetoresistance (MR) measurements. Magnetometry of samples from different regions of the boule exhibited no detectable inhomogeneities. MR measurements[8] utilized standard, four-point contacts made with silver paint on samples that are typically $2\times1\times1$ mm^3. Magnetization M and susceptibility χ measurements were made in a Quantum Design PPMS system equipped with a 9 T superconducting solenoid. The trapped flux in the solenoid ($\sim$15 Oe) was monitored and field values have been adjusted accordingly. The platelets used for magnetometry are similar in shape to those used for resistance measurements and weight 4 to 8 mg. The magnetization measurements reported herein utilize fields applied along the easy axis of the crystals, which is along the a axis within the layered structure.

Figure 1 shows the transitions T_C and T^* that appear in the low-field M vs T data. Besides the Curie transition at 116 K, the additional T^* transition at 287 K also appears in Fig. 1 in 15 Oe, but there is no remanence ($M=O$ for $H<1$ Oe). M forms a plateau of low magnitude below each transition. For the Curie transition this is indicative of a domain state rather than a saturation state, as will be discussed later. Figure 2 illustrates the magnetization above and below T^*, which shows paramagnetic and ferromagnetic responses, respectively. Below T^* the remanent moment is barely nonvanishing at $\sim$0.5 mμ_B/Mn, and the coercive field is $<$10 Oe. Above 10 Oe, M increases linearly with H, as for a paramagnetic response superimposed on a saturated ferromagnetic signal. This saturated ferromagnetic component only represents $\sim$0.1% volume fraction of the sample and therefore can be considered as originating from an impurity phase. The inset of Fig. 2 shows a TEM micrograph of the sample (with the c axis in the plane of the picture). Two intergrowths are easily seen in an otherwise perfect crystal.

While neutron diffraction has previously identified the long-range order (LRO) ferromagnetic state below T_C with fully developed magnetic moments on the Mn sites, it fails to detect Mn moments above T_C.[9] This could be either because their values are small (at 0.1% volume fraction) or because the length scale of the magnetic scattering is too short to be detected. Below T_C the neutron powder-diffraction experiments show that the magnetic coherence length is larger than $\sim$200 Å, i.e., it is resolution limited. (Above T_C, it is not possible to place a quantitative value on the coherence based on the neutron-diffraction scans reported since no magnetic moment was refined.)

An effort was made to extract an experimental magnetization exponent below T^* for the impurity phase. Within 10% of T^*, $M(H=15$ Oe$)$ scales as $(1-T/T^*)^\beta$, with $\beta=0.25\pm0.02$, as shown in Fig. 3, for which T^* was also a fitting parameter. (The same values are observed in 30 Oe. $T^*$and β have correlated errors of ±1 K and ±0.03, respectively, for statistical confidence levels $>$99%.) The β value coincides, within experimental error, with that of the critical magnetization exponent ($3\pi^2/128=0.231$) reported for the finite-size 2D XY model.[11] Similar experimental values have been reported for ultrathin ferromagnetic films with in-plane magnetic anisotropy,[12] as well as $Sr_2CuO_2Cl_2$,[13] a 2D Heisenberg antiferromagnet. In theory, the 2D XY model should not exhibit LRO at finite T, but ordering is permitted once the symmetry is broken, by either a finite-size effect, or the presence of a magnetic field, or a weak in-plane fourfold anisotropy anticipated from the crystal structure (that would yield nonuniversal scaling exponents), or any other infinitesimal anisotropy. The actual value of the β exponent can

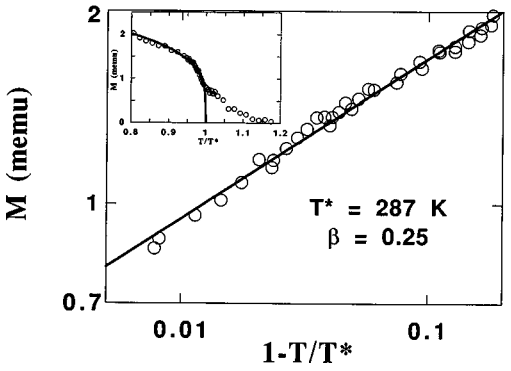

FIG. 3. Log-log plot of M vs reduced temperature showing straight line fit to T^* = 287 K and $\beta=0.25\pm0.02$ within 10% of T^*. M vs T/T^* is displayed in the inset along with the power-law fit. The tail extends to 15% above T^*.

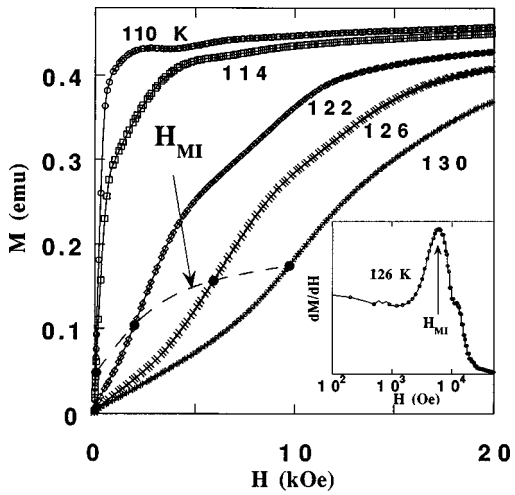

FIG. 4. M vs H for $La_{1.2}Sr_{1.8}Mn_2O_7$ (sweeping up and down in field) at several temperatures below and above T_C. The dashed line, denoted H^{MI}, identifies the field at which the differential susceptibility peaks (see the inset) and this corresponds to the MI transition in the conduction.

also be influenced by the fact that the transition is broadened (see Fig. 3 inset). And, finally, it is possible that double-exchange ferromagnets form different universality classes than traditional magnets because of their fluctuating valence states that are not described in the Hamiltonians of the standard scaling models.

The small (~0.1%) volume fraction and the two-dimensional β analysis combined with the TEM results indicate that the intergrowths (for which $n \neq 2$) are the likely cause of the T^* transition. We can also speculate that intergrowths are present in the $x=0.3$ sample of Ref. 10 because the samples in both studies were synthesized similarly, and the M-H behavior in Ref. 10 for $T < T^*$ are similarly indicative of a trace impurity, rather than intrinsic 2D ordering as implied therein. Intergrowths might even be more prevalent in that study and responsible for the broad and weak slope reversal reported for ρ_{ab} at T^*.

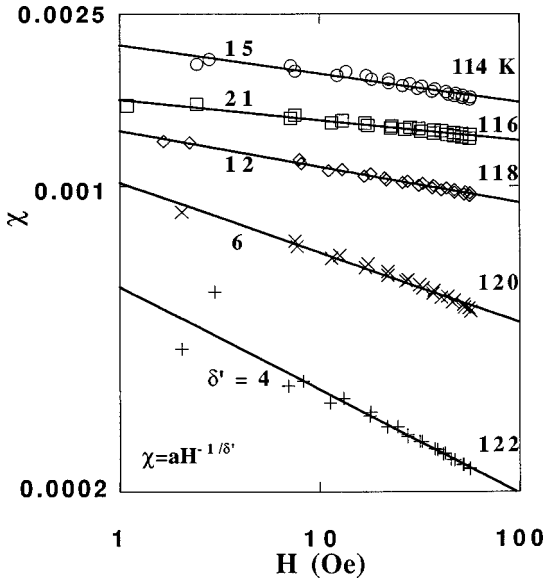

FIG. 5. Log-log plot of χ vs H for single-crystal $La_{1.2}Sr_{1.8}Mn_2O_7$ near T_C denoting δ' values.

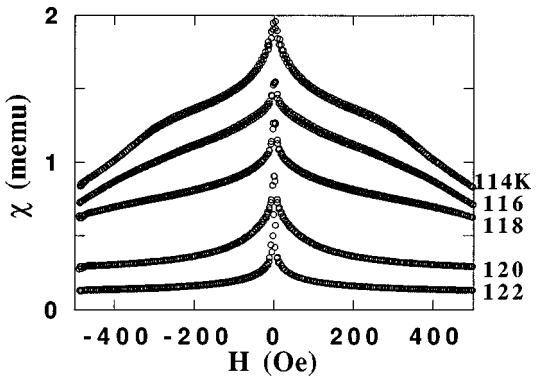

FIG. 6. The χ vs H data on a linear scale as used in Fig. 5.

Now we turn our attention to the Curie transition at 116 K. Figures 4, 5, and 6 show M and χ vs H for the specified temperatures. M vs H is initially linear both above and below T_C, with no remanence apparent, but with slopes that increase on cooling. Above T_C (see, e.g., the 126 K data in Fig. 4) the linear region is followed by an inflection point, denoted H_{MI}, which tracks the field enhancement of the concomitant MI and Curie transitions. This same trend in H_{MI} was reported in Refs. 8 and 9 from the resistivity data for this composition. Here we define H_{MI} as the field at which the susceptibility peaks (see Fig. 4 inset). The H-T phase diagram is summarized in Fig. 7, which also shows the saturation field and the two neutron data points (closed symbols) from Ref. 9 that delineate the LRO and SRO regions.

χ vs H diverges as a power law at low field (see Figs. 5 and 6). We represent this behavior phenomenologically as $\chi \sim H^{-1/\delta}$. This implies that the approximate linearity of M vs H can be similarly represented as $M \sim H^{1-1/\delta}$. Fitting the low-field χ data indicates that δ' grows at T_C is approached. We find that $\delta' = 4 \pm 1$ at 122 K, which is ~6 K from T_C and $\delta' = 21 \pm 5$ at 116 K, which is within 1 K of T_C. Below T_C the value of δ' may simply reflect the domain state. At T_C however, scaling theory should apply. Standard scaling theory would yield $M \sim H^{1/\delta}$ and $\chi \sim H^{1/\delta - 1}$, with $\delta = 15$ for a 2D system (XY or Ising). Thus, our experimental power laws for M and χ seem to differ in sign and functional form from their traditional values. However, within the theory of

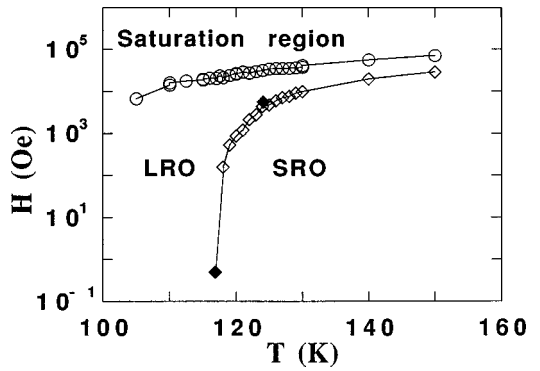

FIG. 7. H-T phase diagram of $La_{1.2}Sr_{1.8}Mn_2O_7$. The saturation fields (open circles) and the M_{MI} (open diamonds) from magnetization data, while the closed diamonds indicate the onset of LRO in the neutron-scattering refinements of Ref. 9.

planar degenerate systems,[14] the exponent $1/\delta = k_B T_C/4\pi J$ for the XY model. Therefore, we can interpret our unusual δ' exponent as indicating $k_B T_C/J \approx 12$, which is comparable to values found for similar high-spin 2D systems.[15] The interesting point here is that the fluctuations near T_C could be 2D while the transition itself is 3D (in the sense that ρ_{ab} and ρ_c both exhibit MI behavior at T_C). Again, as was mentioned above, nonstandard scaling behavior might be possible in double-exchange ferromagnets (and in this regard unusual ferromagnetic and antiferromagnetic 2D fluctuations extending well above T_C for $x=0.4$ samples recently were reported by Perring *et al.*[16] in neutron-scattering experiments).

In summary, 2D behavior is exemplified in single crystals of $La_{1.2}Sr_{1.8}Mn_2O_7$, the 40% doped, two-layer variant of the CMR perovskite manganites. This material exhibits LRO and an MI transition at $T_C = 116$ K and a susceptibility divergence described phenomenologically by $\chi = H^{-1/\delta'}$ with $\delta' = 21 \pm 5$ at T_C. The material also exhibits an extrinsic Curie transition attributed to $\sim 0.1\%$ volume fraction of intergrowths at $T^* = 2.47 T_C$ and for which M scales as $(1 - T/T^*)^{\beta}$, with $\beta = 0.25 \pm 0.02$. These results provide a new perspective on the layered manganites, in contrast to that proposed earlier. It is of the utmost importance to pursue these divergent viewpoints in order to provide theorists with a baseline for describing the physics of this fascinating class of magnetic materials.

We thank D. Golosov, K. E. Gray, and V. L. Pokrovsky for valuable discussions. This work was supported by the U.S. Department of Energy, BES-MS, and ER, LTR under Contract No. W-31-109-ENG-38 and by the NSF OSTC under Contract No. DMR 91-20000 (DNA).

*Present address: Seagate Technology, Bloomington, MN 55435.
†Present address: University of Illinois, Urbana-Champaign, IL.
‡Present address: Neutron Science Center, Los Alamos National Laboratory, NM.

[1] R. van Helmolt, J. Wecker, B. Holzapfel, L. Schultz, and K. Samwer, Phys. Rev. Lett. **71**, 2331 (1993).
[2] M. McCormack, S. Jin, T. H. Tiefel, R. M. Fleming, J. M. Phillips, and R. Ramesh, Appl. Phys. Lett. **64**, 3045 (1994).
[3] J. F. Mitchell, D. N. Argyriou, C. D. Potter, D. G. Hinks, J. D. Jorgensen, and S. D. Bader, Phys. Rev. B **54**, 6172 (1996).
[4] P. E. Schiffer, A. P. Ramirez, W. Bao, and S.-W. Cheong, Phys. Rev. Lett. **75**, 3336 (1995).
[5] C. Zener, Phys. Rev. **81**, 440 (1951).
[6] See Fig. 2 of J. M. De Teresa, M. R. Ibarra, J. Garcia, J. Blasco, C. Ritter, P. A. Algarabel, C. Marquina, and A. del Moral, Phys. Rev. Lett. **76**, 3392 (1996).
[7] Y. Moritomo, A. Asamitsu, H. Kuwahara, and Y. Tokura, Nature (London) **380**, 141 (1996).
[8] J. F. Mitchell, D. N. Argyriou, J. D. Jorgensen, D. G. Hinks, C. D. Potter, and S. D. Bader, Phys. Rev. B **55**, 63 (1997).
[9] D. N. Argyriou, J. F. Mitchell, J. B. Goodenough, O. Chmaissem, S. Short, and J. D. Jorgensen, Phys. Rev. Lett. **78**, 1568 (1997).
[10] T. Kimura, Y. Tomioka, H. Kurahawa, A. Asamitsu, M. Tamura, and Y. Tokura, Science **274**, 1698 (1996).
[11] S. T. Bramwell and P. C. W. Holdsworth, J. Phys. Condens. Matter **5**, L53 (1993).
[12] Z. Q. Qiu, J. Pearson, and S. D. Bader, Phys. Rev. B **49**, 8797 (1994); C. H. Back, Ch. Wursch, A. Vaterlaus, U. Ramsperger, U. Maier, and D. Pescia, Nature (London) **378**, 597 (1995).
[13] M. Greven, R. J. Birgeneau, Y. Endoh, M. A. Kastner, M. Matsuda, and G. Shirane, Z. Phys. B **96**, 465 (1995).
[14] A. Z. Patashinskii and V. L. Pokrovskii, *Fluctuation Theory of Phase Transitions* (Pergamon, Oxford, 1979).
[15] L. J. De Jongh, P. Bloembergen, and J. H. P. Colpa, Physica (Amsterdam) **58**, 305 (1972).
[16] T. G. Perring, G. Aeppli, Y. Moritomo, and Y. Tokura, Phys. Rev. Lett. **78**, 3197 (1967).